

CHAPTER 5 - SYMMETRY AND VIBRATIONAL SPECTROSCOPY

5.1 Potential Energy Diagrams

The energy of a molecule can be approximated as $E = E_{\text{rot}} + E_{\text{vib}} + E_{\text{elec}} + E_{\text{tran}} + E_{\text{spin}} + E_{\text{nuc}}$. If we make the approximation that the wavefunction is separable, then the problem can be reduced to several smaller tasks. This amounts to the assumption of the Born-Oppenheimer approximation, which permits the nuclear and electronic motions to be analyzed separately. In fact, this approximation breaks down, and leads to the Jahn-Teller phenomenon and other vibronic effects. Let us now address the pure vibrational problem. Exchange of energy between a molecule and the electromagnetic field occurs when $h\nu = \Delta E$, where ΔE is the difference between initial and final quantized states. In terms of energies

$$\nu = \frac{c}{\lambda} \frac{\text{cm/sec}}{\text{cm}} = \text{Hz} \quad \bar{\nu} = \frac{1}{\lambda} = \frac{\nu}{c} = \text{cm}^{-1}$$

Infrared absorption spectra usually cover the range 200-4000 cm^{-1} or 50-2.5 micrometers (microns). The conversion factor 1 e.v. = 8066 cm^{-1} or 23 kcal/mole is also useful to remember. Translational energies are about 200 cm^{-1} at room temperature and rotational energies are 1-100 cm^{-1} . Most infrared spectrometers provide the spectrum in the form of % transmittance vs. wavenumber. Transmittance spectra tend to emphasize weak absorptions in the spectrum. Spectra of the same sample recorded at different concentrations will have different relative peak heights, when displayed as % transmittance. Conversion to absorbance spectra (absorbance = $-\log_{10}$ (transmittance)) is an option available on most spectrometers. Absorbance spectra should be used whenever peak ratios or concentration information is desired (*e.g.*, in kinetics, where the decrease or increase of concentration must be monitored). The other important aspect to IR and Raman spectroscopy is that the time scale of the measurement amounts to the time it takes for a vibration (\sim 0.1 psec). Even rapidly isomerizing species show distinct vibrational spectra in contrast to slower techniques, such as NMR spectroscopy.

Figure 5.1 shows the vibrational potential energy surface for a harmonic oscillator (A)

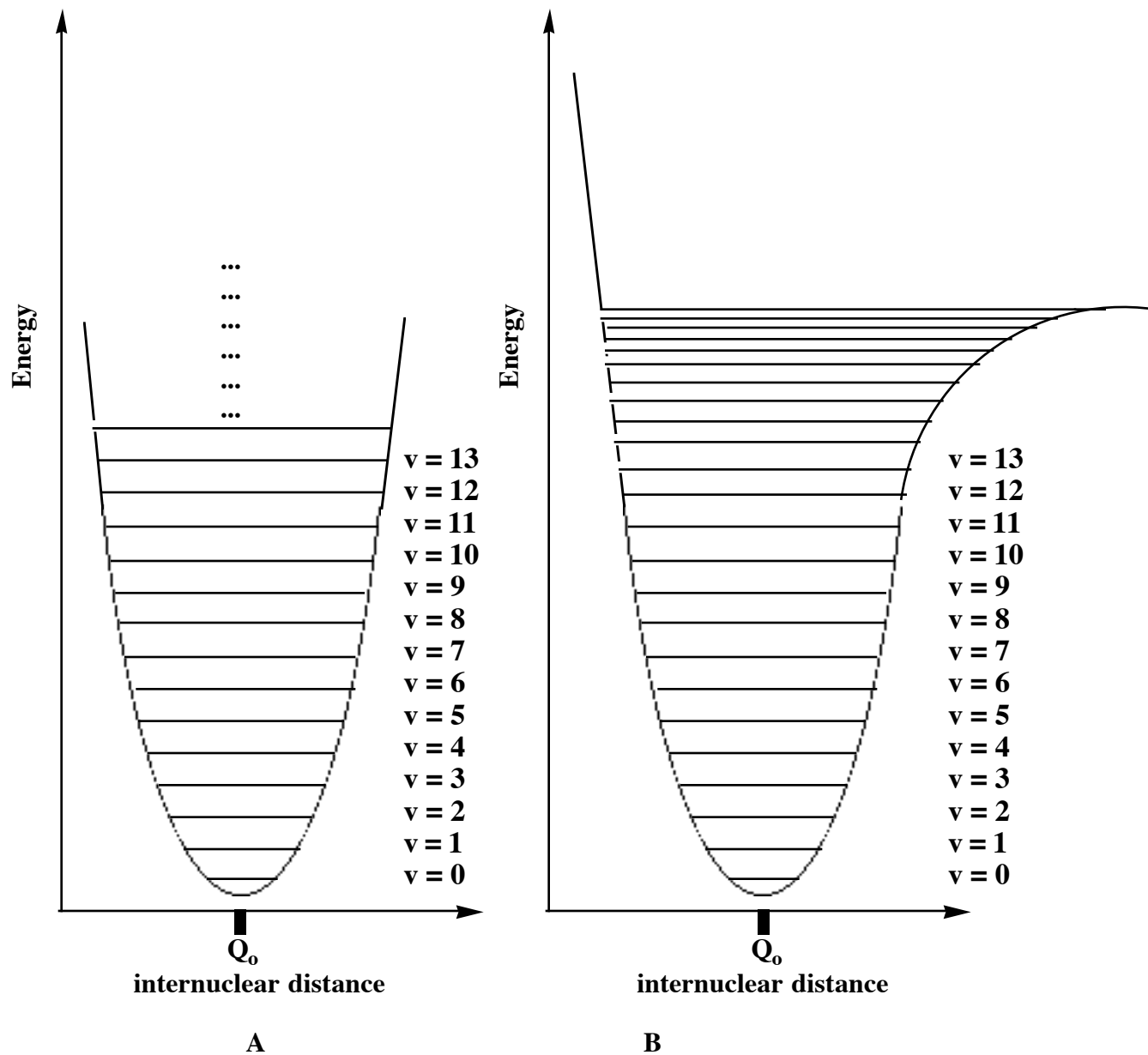


Figure 5.1 Potential energy vs. internuclear distance diagrams for a diatomic molecule which behaves like an ideal harmonic oscillator (A) and that observed for a real molecule (B). Q_0 denotes the equilibrium internuclear distance and v the vibrational quantum numbers for the stretching vibration.

and for a nonideal diatomic molecule (B). These plots depict how the total electronic energy of the molecule varies as the internuclear distance varies away from its internuclear values Q_0 . In the simplest approximation the bond joining the atoms is assumed to behave as a spring. In polyatomics, where the nuclear motion may be complex, it is still assumed that the overall

vibrational motion along the coordinate Q can be described with a spring-like force. Then the restoring force, F , is given by Hooke's Law:

$$F = k(Q_0 - Q)$$

And by integration the energy E is given by:

$$E = \frac{1}{2}k (Q_0 - Q)^2$$

This equation generates the parabolic surface of Figure 5.1 A. The nuclei are constrained to move on this potential surface, and solution of the Schrödinger wave equation yields the quantized vibrational energy levels with energies.

$$E_v = h\nu (v + \frac{1}{2})$$

Here v is vibrational quantum number 0, 1, 2, ... The frequency of vibration ν is given by

$$\nu = \frac{1}{2\pi} \sqrt{\frac{k}{\mu}}$$

where k is the bond force constant and μ is the reduced mass for two nuclei of masses m_1 and m_2 .

$$\frac{1}{\mu} = \frac{1}{m_1} + \frac{1}{m_2}$$

This yields the quantized vibrational level scheme shown in Figure 5.1 A. Because transitions between the $v = 0$ and $v = 1$ levels dominate in infrared or Raman spectroscopy, the harmonic oscillator description provides a useful approximation for real molecules, 5.1 B, near the bottom of the potential well.

There are several predictions of the harmonic oscillator model. First, the frequency ν becomes smaller as μ increases (heavier atoms), or as k decreases. The force constant k , which represents the second derivative or curvature of the potential surface of Q_0 , often parallels bond strengths, D_0 ; however, there's not necessarily a correlation between the two. These facts are illustrated by the data in Table 5.1 for the halogens.

Table 5.1. Vibrational frequencies $\bar{\nu}$, Force Constants, k , and Dissociation Energies, D_0 for the Halogens

	$\bar{\nu}$, cm^{-1}	k (mdyn/Å)	D_0 kcal/mole
F_2	892	4.45	37
Cl_2	546	3.19	58
Br_2	319	2.46	46
I_2	215	1.76	36

5.2 Normal Modes in Polyatomic Molecules

Consider a molecule containing N atoms. Because most of the mass resides in the nuclei, the translational, rotational and vibrational motions of the molecule can be approximated by considering only nuclear motions. This assumption of separability of nuclear motion from that of the electrons amounts to the Born-Oppenheimer approximation. If there are N nuclei, then each nucleus possesses $3N$ degrees of freedom in three dimensional space. Three of these coordinates describe translational motion of the center of mass and three more degrees of freedom describe rotations around the center of mass. For linear molecules only two degrees of freedom are needed to describe rotations. The remaining $3N-6$ degrees of freedom ($3N-5$ if linear) describe vibrations. Symmetry species of translations, rotations, and vibrations can be determined by considering the character of the representation spanned by Cartesian vectors localized on each atom. For example, consider the PtCl_4^{2-} ion of Figure 5.2, with the z axis assumed to emerge from the plane of the page for each atom.

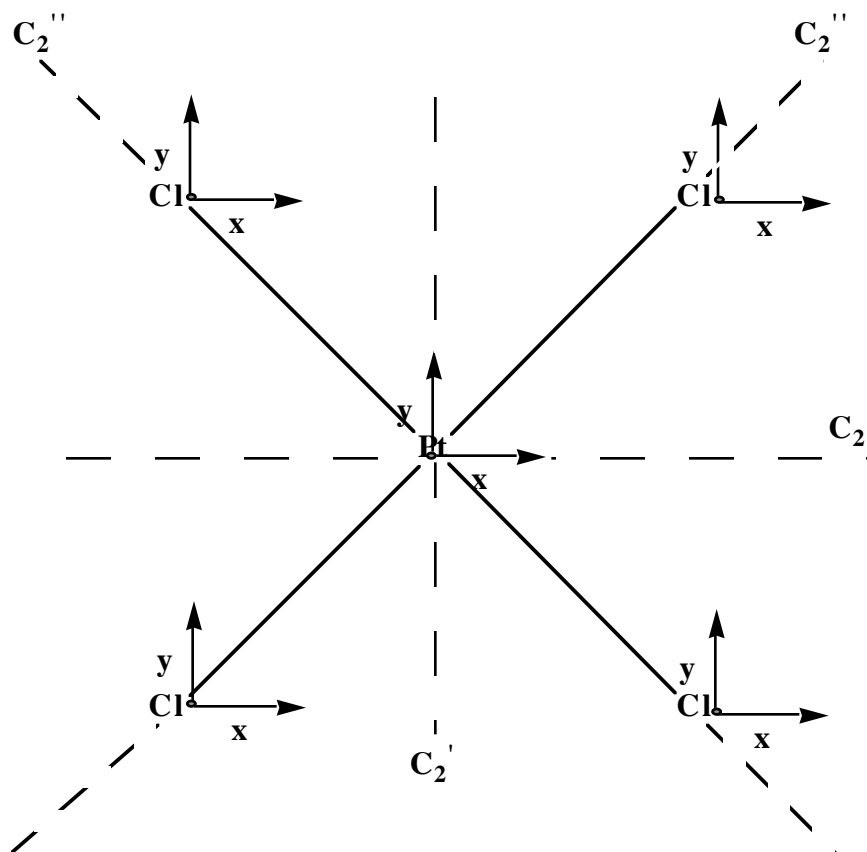


Figure 5.2 Choice of Cartesian coordinate system for PtCl_4^{2-} - \square_v is in the xz and yz planes with $2 \square_d$ between these planes.

Although the choice of coordinate system is arbitrary, we choose it so the operations of the D_{4h} group transform the x, y, z vectors into \pm themselves, or else into one another. Recall, that to compute the character for the representation spanned by the $3N$ coordinates, denoted $X(3N)$, you need only sum the diagonal elements of the 15 -dimensional transformation matrix. Under a \hat{C}_4 rotation, for example, the chlorine atoms interchange. No vector from these atoms can go into \pm itself or some fraction thereof. They contribute zero to the character. Similarly, the vectors x and y on Pt go to $+y$ and $-x$, respectively, which together contribute zero to the character. Only z on Pt, which goes into z on a \hat{C}_4 rotation (*i.e.*, is unchanged), contributes a $+1$ to the diagonal of the transformation matrix. So the character for \hat{C}_4 is $+1$. Characters for the other operations appear below.

$$\begin{array}{rcccccccccc}
 & \hat{E} & 2\hat{C}_4 & \hat{C}_2 & 2\hat{C}_2' & 2\hat{C}_2'' & \hat{i} & 2\hat{S}_4 & \hat{\sigma}_h & 2\hat{\sigma}_v & 2\hat{\sigma}_d \\
 \Gamma(3N) & 15 & 1 & -1 & -1 & -3 & -3 & -1 & 5 & 1 & 3 \\
 = & A_{1g} & + A_{2g} & + B_{1g} & + B_{2g} & + E_g & + 2A_{2u} & + B_{1u} & + 3E_u
 \end{array}$$

Now remove from this 15-dimensional reduced representation the translations, which transform like $x, y, z = A_{2u} + E_u$ and the rotations $R_x, R_y, R_z = E_g + A_{2g}$ to yield the $\Gamma(3N-6)$ vibrations of the molecule $= A_{1g} + B_{1g} + B_{2g} + A_{2u} + B_{1u} + 2E_u$. This list comprises the normal modes of vibration. They describe the symmetry representations for all possible vibrational motions or vibrational wavefunctions of the PtCl_4^{2-} ion. Any motion of the molecule that leaves the center of mass fixed, and which does not rotate the molecule, can be represented as a superposition of the normal modes of vibration. It is informative to consider the symmetries of the vibrational coordinates and use the projection operator to obtain a visual representation. In the case of PtCl_4^{2-} , there will be an ambiguity in the nature of the E_u vibrations obtained. There are two modes of this symmetry in the list of possible normal modes and the exact nature of each can only be determined by solving the vibrational Hamiltonian. Mixing may occur between the symmetry adapted vibrational coordinates of the same symmetry. This problem goes beyond what simple group theory can determine.

We could solve the symmetry coordinate problem with Cartesian displacements (and subtract out rotations and translations); however, it is customary to use "internal coordinates" that correspond to bond stretches, bends, and torsions. Vibrational motions depicted in the internal coordinate system correspond better to intuitive notions of bond stretching and bending. Unlike the cartesian coordinates, problems arise because the internal coordinates are not always orthogonal and linearly independent. One must be careful to eliminate redundancies that arise in the internal coordinates, and to modify the internal coordinate motions to ensure the center of mass remains fixed. If the center of mass shifts then the motion would not be a pure vibration, but contains some translational motion as well. For example, the four Cl-Pt-Cl angles (Figure 5.3) are not linearly independent. Any three fix the value of the remaining angle in the plane, because all four must sum

to 360° . Thus, only three of the angles are linearly independent. If we attempt to construct four linear combinations from these four angles with the projection operator, then one will be spurious.

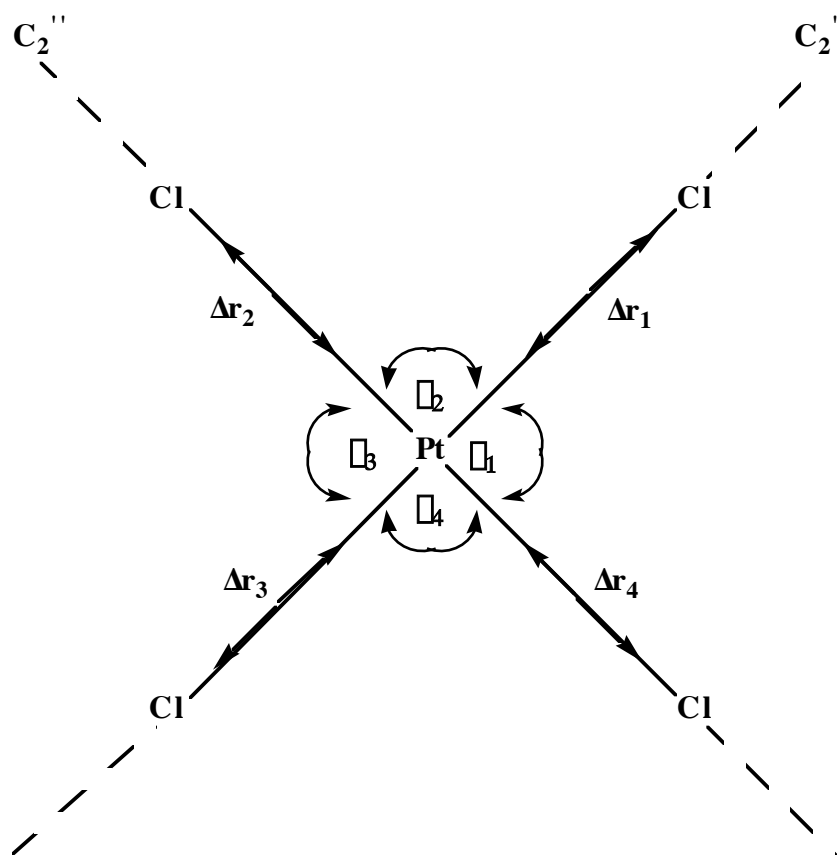


Figure 5.3 Choice of internal coordinate system for PtCl_4^{2-} .

First, consider PtCl_4^{2-} and the set of coordinates for Pt-Cl bond stretching $\Delta r_1, \Delta r_2, \Delta r_3,$ and Δr_4 shown in Figure 5.3. The character of the Pt-Cl bond stretches is:

	E	$2C_4$	C_2	$2C_2'$	$2C_2''$	i	$2S_4$	σ_h	$2\sigma_v$	$2\sigma_d$
$\chi(\text{Pt-Cl})$	4	0	0	0	2	0	0	4	0	2

$= A_{1g} + B_{2g} + E_u$

Using the projection operator, the totally symmetric stretch is found to be

$$P_{a_{1g}}(\Delta r_1) = N(\Delta r_1 + \Delta r_2 + \Delta r_3 + \Delta r_4)$$

At present we won't concern ourselves with normalization conditions.

The B_{2g} coordinate is found by applying $P^{B_{1g}}(\Delta r_1)$ to yield:

	E	C ₄	C ₄ ³	C ₂	C ₂ '	C ₂ '	C ₂ ''	C ₂ ''	i	S ₄	S ₄ ³
$\hat{R}(\Delta r_1)$	Δr_1	Δr_2	Δr_4	Δr_3	Δr_2	Δr_4	Δr_1	Δr_3	Δr_3	Δr_2	Δr_4
$\square(B_{2g})$	1	-1	-1	1	-1	-1	1	1	1	-1	-1
	\square_h	\square_\square	\square_\square	\square_d	\square_d						
$\hat{R}(\Delta r_1)$	Δr_1	Δr_2	Δr_4	Δr_1	Δr_3						
$\square(B_{2g})$	1	-1	-1	+1	+1						

$$PB_{2g}(\Delta r_1) = N(\Delta r_1 + \Delta r_3 - \Delta r_2 - \Delta r_4)$$

Also for the degenerate stretching vibrations.

$$\square^{Eu}(\Delta r_1) = N(\Delta r_1 - \Delta r_3)$$

The other partner may be generated by application of \hat{C}_4 .

$$N\hat{C}_4(\Delta r_1 - \Delta r_3) = N(\Delta r_2 - \Delta r_4)$$

The orthogonal linear combination derived from the sum and difference of the preceding pair is normally used.

$$N'[\Delta r_1 + \Delta r_2 - \Delta r_3 - \Delta r_4]$$

$$N'[\Delta r_1 + \Delta r_4 - \Delta r_2 - \Delta r_3]$$

These stretching vibrations are depicted in Figure 5.4. It is important to reemphasize that the center of mass must not move during a normal vibration. Otherwise the motion would include some translational motion and not be a pure vibration. For the degenerate e_u stretching vibration, some motion of the central Pt must be added, as shown in the figure, so the center of mass remains fixed. It is always required that no center of mass motion (a translation) occur in a pure vibration, and this condition must always be applied to the SALC one obtains.

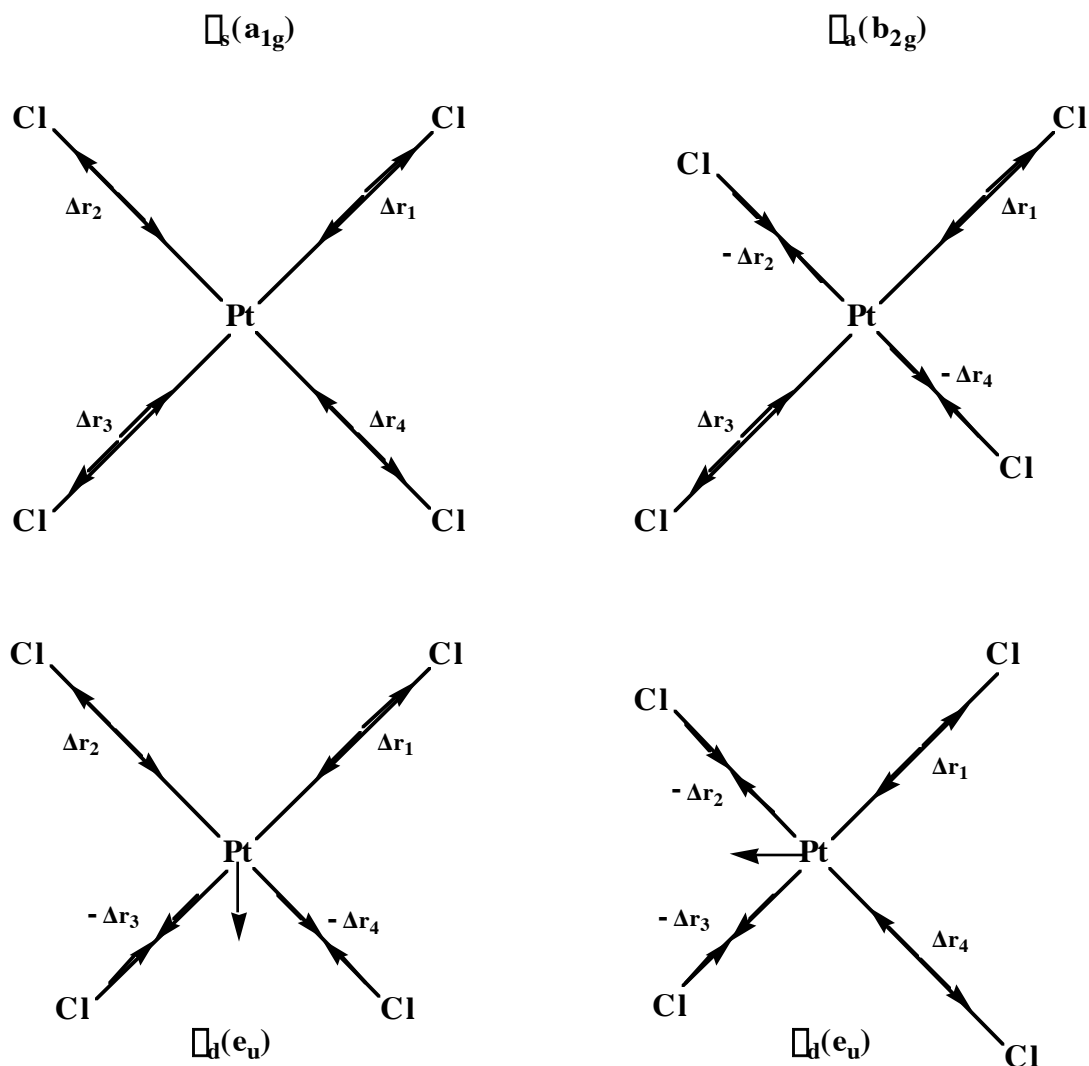


Figure 5.4 Symmetry adapted linear combinations of the a_{1g} , b_{2g} , and e_u Pt-Cl stretching vibrations in $PtCl_4^{2-}$.

The $\Gamma_{a_{1g}}$ and $\Gamma_{b_{2g}}$ vibrations are often called the symmetric and antisymmetric stretches, Γ_s and Γ_a , in MX_4 complexes. They usually occur at similar energies with $\Gamma_s > \Gamma_a$. The E_u mode is called Γ_d and can mix with the E_u angle deformation (*vide infra*). In these complexes, $\Gamma_d > \Gamma_s > \Gamma_a$. As is always the case, the frequencies shift to lower energies as the mass of the halide increases. Metal-ligand stretching vibrations in transition metal complexes usually occur below 450 cm^{-1} . The motions that involve bending or deformation of metal-ligand bond angles fall at even lower frequencies.

	$\Gamma_s(a_{1g})$	$\Gamma_a(b_{2g})$	$\Gamma_d(e_u)$
PtCl ₄ ²⁻	330 cm ⁻¹	312 cm ⁻¹	313 cm ⁻¹
PtBr ₄ ²⁻	208	194	227
PtI ₄ ²⁻	155	142	180

Bending and Angle Deformation Vibrations. Next consider the bending vibrations Γ_1 - Γ_4 of PtCl₄²⁻ shown in Figure 5.3. The characters for the representation are:

	E	2C ₄	C ₂	2C ₂ '	2C ₂ ''	i	2S ₄	Γ_h	2 Γ_v	2 Γ_d
$\Gamma(\Gamma)$	4	0	0	2	0	0	0	4	2	0

$$= a_{1g} + b_{1g} + e_u$$

Recall that one representation will prove to be redundant, because if Γ_1 , Γ_2 , and Γ_3 are known then Γ_4 is fixed by the requirement that their sum totals 360°. Application of the projection operator for the a_{1g} vibration yields:

$$a_{1g}(\Gamma) = N(\Gamma_1 + \Gamma_2 + \Gamma_3 + \Gamma_4)$$

However, it is impossible for all four angles to increase simultaneously, and this a_{1g} "bending vibration" is a nonsensical consequence the internal coordinate redundancy. This arises because Γ_1 Γ_4 were not linearly independent.

The b_{1g} and e_u SALC's are genuine symmetry coordinates for vibrations. Application of the projection operator yields:

	E	C ₄	C ₄ ³	C ₂	C ₂ '	C ₂ '	C ₂ ''	C ₂ ''	i	S ₄	S ₄ ³	Γ_h	Γ_v	Γ_v	Γ_d	Γ_d
R(Γ_1)	Γ_1	Γ_2	Γ_4	Γ_3	Γ_1	Γ_3	Γ_4	Γ_2	Γ_3	Γ_2	Γ_4	Γ_1	Γ_1	Γ_3	Γ_4	Γ_2

$$P^{b1g}(\Gamma_1) = N(\Gamma_1 + \Gamma_3 - \Gamma_2 - \Gamma_4)$$

For the e_u mode we obtain ($\Gamma_1 - \Gamma_3$) and its partner ($\Gamma_2 - \Gamma_4$). These bending vibrations are depicted in Figure 5.5. Note the added motion of Pt necessary to leave the center of mass fixed in the e_u mode.

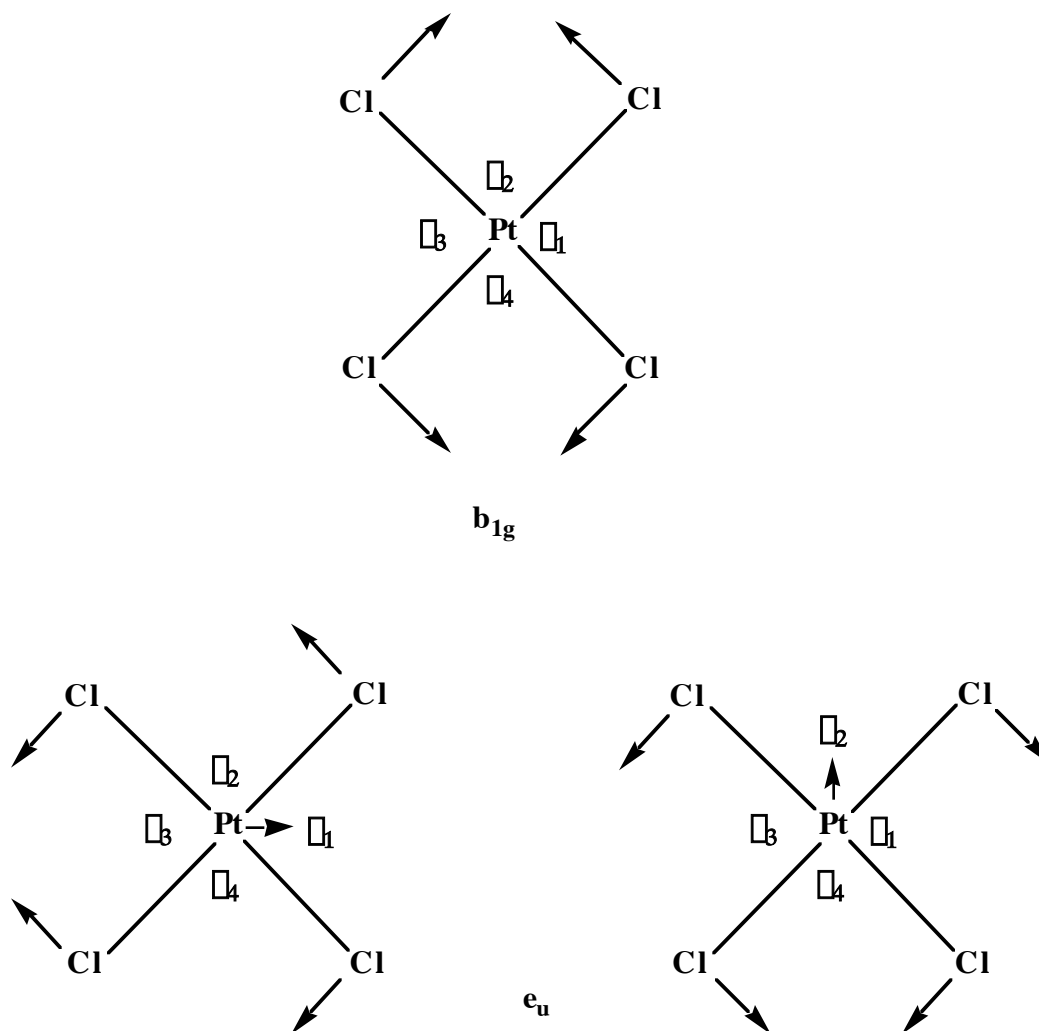


Figure 5.5 Sketch of the b_{1g} and e_u bending vibrations of PtCl_4^{2-} .

Finally, consider the out-of-plane bending vibrations. As yet, the a_{2u} and b_{1u} vibrational modes in the complete list of $3N-6$ vibrations are not accounted for by the in plane bends and stretches. We anticipate that the out-of-plane motions should account for the missing vibrations. The out of plane bends can be depicted by a vector displacement perpendicular to the plane of the molecule for each of the four chloride ligands. A + to denotes displacement above the plane for each chlorine atom, and a - denotes displacement below the plane. Since this spans a four

dimensional representation, and since only a_{2u} and b_{1u} are missing, it is clear that the two extra dimensions must arise from redundancies in the coordinates.

	4	0	0	0	2	0	0	4	0	2
	E	$2C_4$	C_2	$2C_2'$	$2C_2''$	i	$2S_4$	σ_h	$2\sigma_v$	$2\sigma_d$
$\Gamma(+)$	4	0	0	0	-2	0	0	-4	0	2

$= a_{2u} + b_{1u} + e_g$ The e_g representation must be redundant, because only the a_{2u} and b_{1u}

vibrations are left. Application of the projection operator for them yields:

	E	C_4	C_4^3	C_2	C_2'	C_2'	C_2''	C_2''	i	S_4	S_4	σ_h	σ_v	σ_v	σ_d	σ_d
$\hat{R}(+1)$	+1	+2	+4	+3	-4	-2	-1	-3	-3	-2	-4	-1	+4	+2	+1	+3
$\Gamma(a_{2u})$	1	1	1	1	-1	-1	-1	-1	-1	-1	-1	-1	1	1	1	1
$\Gamma(b_{1u})$	1	-1	-1	1	1	1	-1	-1	-1	1	1	-1	-1	-1	1	1

$$P^{a_{2u}}(+1) = 2(+1) - 2(-1) + 2(+2) - 2(-2) + 2(+3) - 2(-3)$$

$$+ 2(+4) - 2(-4)$$

$$= 4\{(+1) + (+2) + (+3) + (+4)\}$$

$$P^{b_{1u}}(+1) = 4\{(+1) + (-2) + (+3) + (-4)\}$$

Calculating these linear combinations uses the relation that $-(+1) = +(-1)$. In other words, minus a positive displacement of atom #1 is the same as a negative displacement of the same atom. The out of plane vibrations are sketched in Figure 5.6.

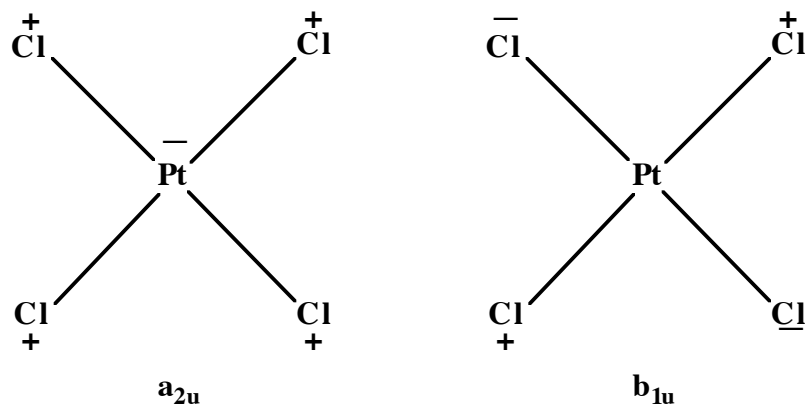


Figure 5.6 Sketch of the a_{2u} and b_{1u} bending vibrations of $PtCl_4^{2-}$.

For PtCl_4^{2-} , the complete set of observable vibrations are:

	Stretches		in-plane bends		out-of-plane bends
$\Gamma_6(e_u)$	$\Gamma_1(a_{1g})$	$\Gamma_4(b_{2g})$	$\Gamma_2(b_{1g})$	$\Gamma_7(e_u)$	$\Gamma_3(a_{2u})$
$\Gamma_d(\text{Pt-Cl})$	$\Gamma_s(\text{Pt-Cl})$	$\Gamma_h(\text{Pt-Cl})$	$\Gamma_d(\text{PtCl}_2)$	$\Gamma_d(\text{PtCl}_2)$	Γ
313 cm^{-1}	330 cm^{-1}	312 cm^{-1}	171 cm^{-1}	165 cm^{-1}	147 cm^{-1}

The $\Gamma_s(b_{1u})$ mode is not IR or Raman active, as will be discussed and cannot be observed.

Selection Rules in Infrared and Raman Spectroscopy. The quantum mechanical solution of the harmonic oscillator problem yields the vibrational wavefunctions:

$$\psi_i(\xi) = N_i e^{-(\xi/2)\alpha_i^2} H_v\left(\sqrt{\alpha_i}\xi\right)$$

- where N_i = normalization constant
 ξ = vibrational quantum # in the i th normal coordinate
 α_i = $2\pi(\nu_i/h)$ (ν_i = frequency of i th normal mode)
 ξ_i = normal coordinate displacement of i 'th vibration
 $H_\nu(\xi)$ = Hermite Polynomials
- $H_0(\xi) = 1$
 $H_1(\xi) = 2\xi$
 $H_2(\xi) = 4\xi^2 - 2$
 $H_3(\xi) = 8\xi^3 - 12\xi$, etc.

In polyatomic molecules, each vibrational symmetry coordinate is assumed to behave like a harmonic oscillator for displacements along the vibrational coordinate ξ_j . For any vibrational mode, the ground state symmetry ($v = 0$) needs to be considered separately from excited vibrational levels ($v \neq 0$). The ground state vibrational level $\psi_i(0) \approx e^{-(\xi)^2}$, behaves like the totally symmetric representation, whereas $\psi_i(\xi)$ has symmetry of $\xi^v = [\Gamma_1(\xi)]^v$. This results because the vibrational

coordinate appears to the v power in the various H_v , and $e^{-\text{const}\nu^2}$ is totally symmetric. Squaring any irreducible representation always generates the totally symmetric direct product.

Because of the mathematical properties of the harmonic oscillator integrals, only $v \rightarrow v + 1$ transitions are allowed. Typically, only the $v = 0$ to $v = 1$ transitions are observed in infrared spectra. This is because most molecules in a macroscopic sample reside in the $v = 0$ level, with only a few percent excited by the ambient thermal energy to $v = 1, v = 2, \dots$. Thermal population of upper vibrational levels can be calculated from Boltzmann statistics.

$$N(v > 0)/N(v = 0) = \exp[-v(h\nu)/kT]$$

Furthermore, the lower part of the potential surface closely resembles a harmonic oscillator and the $v = 1$ to $v = 2$ transitions are identical in energy to the $0 - 1$ transition for all practical purposes.

The IR allowed transitions are given by the dipole moment integrals $\langle a_{1g} | \hat{d}(e_u) | \nu_i \rangle$ and $\langle a_{1g} | \hat{d}_z | \nu_i \rangle$. The a_{1g} part represents the totally symmetric ground state. For PtCl_4^{2-} , the symmetry of the relevant dipole moment operators from the D_{4h} character table are $\hat{d}_{x,y} = e_u$ and $\hat{d}_z = a_{2u}$. Therefore ν_i , the vibrational mode excited, must be e_u or a_{2u} in order to be dipole allowed. We conclude that only the $\nu_{d(e_u)}$ stretch in PtCl_4^{2-} would be observed in the IR spectrum. The x,y character of the dipole moment for this transition means that the field of the oscillating electric vector of the IR radiation must lie in the x,y or molecular plane, in order to excite the transition. This can be tested experimentally with a crystal of known structure and polarized IR radiation. For the bending vibrations, both e_u and a_{2u} should be observed in the IR spectrum. One should be polarized in the molecular plane, and the other polarized perpendicular to it.

Fortunately, ground state vibrations forbidden in the IR spectrum may be observed by two other techniques - Raman and fluorescence spectroscopy. Raman spectroscopy relies on the inelastic scattering process between a photon and a molecule depicted in Figure 5.7. Although the scattered light may differ from the incident light by $\pm E_{\text{vib}}$, the so called Stokes scattering ($h\nu = E_{\text{vib}}$) is more intense. Maxwell-Boltzmann statistics can be used to estimate the intensity of the two types of scattered radiation, because the Stokes line originates in the $\nu = 0$ ground state level, while

the anti-Stokes Raman scattered light ($h\nu + E_{\text{vib}}$) originates from the thermally populated molecules in the $\nu = 1$ vibrational level.

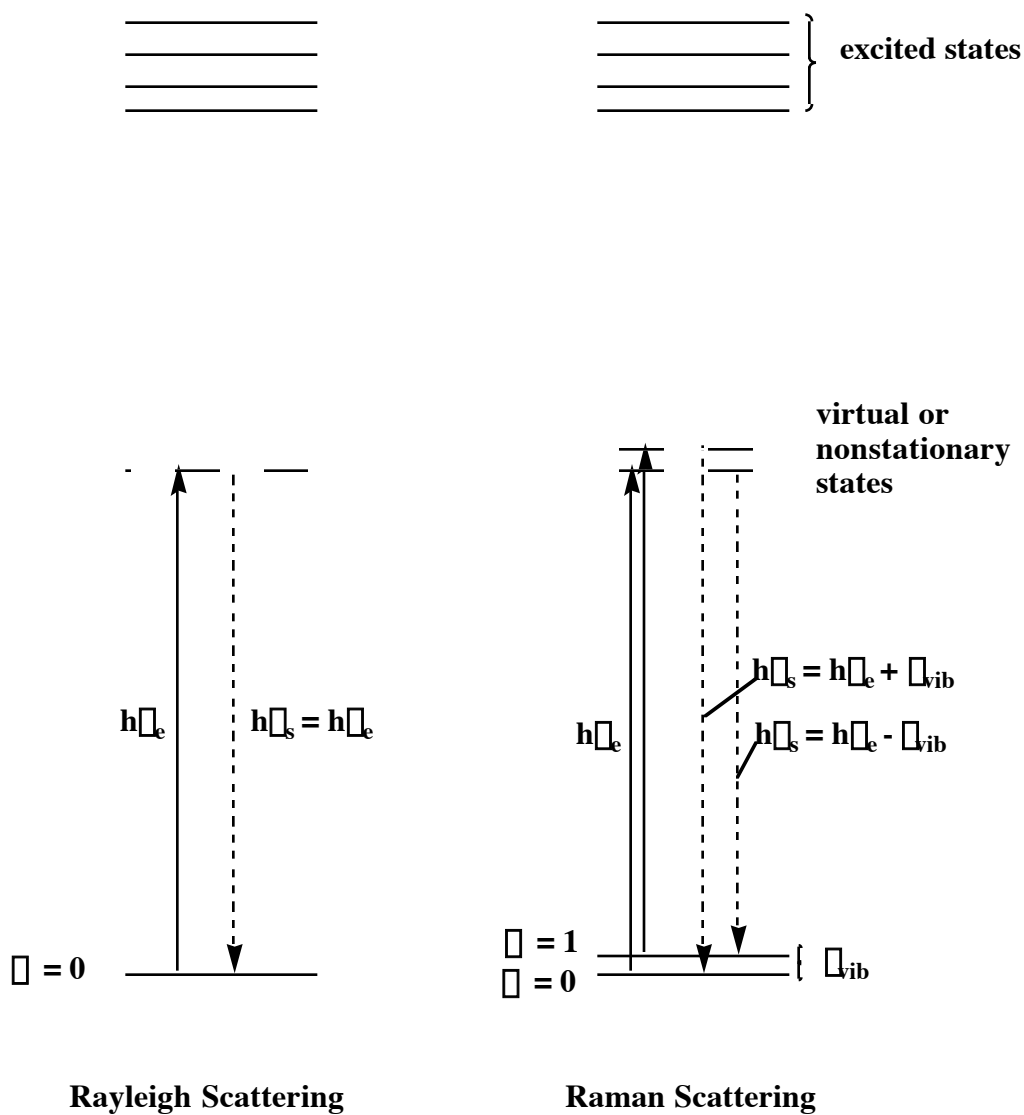


Figure 5.7 Description of Rayleigh scattering, where the scattered light is of the same frequency of the incident light, and Raman scattering, where the scattered light differs by the simultaneous absorption or release of vibrational energy to the scattered light photon.

Raman scattering is only 10^{-4} - 10^{-5} that of elastic Rayleigh scattering for most samples. Intense light sources (lasers) are required in Raman spectroscopy. Detection of the weak intensity Raman scattering, which occurs within 50 - 4000 cm^{-1} of the intense Rayleigh scattered photons, also

requires a good monochromator to separate the various frequency components, and a sensitive photon detector. Because a molecule is bombarded with $\sim 10^5$ photons for every Raman scattered photon, thermal and photochemical decomposition are a concern for samples that may absorb at the laser frequency. Flow cells, rotating samples, and low temperatures have been used to overcome these problems. One must always be concerned with spurious signals from decomposition products in Raman spectroscopy.

Raman spectroscopy has a $\Delta v = \pm 1$ selection rule like infrared spectroscopy. Raman scattering depends on the polarizability tensor α .

$$\alpha \approx \begin{pmatrix} \alpha_{xx} & \alpha_{xy} & \alpha_{xz} \\ \alpha_{xy} & \alpha_{yy} & \alpha_{yz} \\ \alpha_{zx} & \alpha_{yz} & \alpha_{zz} \end{pmatrix}$$

Tensors are required when a system does not respond like a scalar quantity. In Raman scattering, an incident photon scatters in various directions with different probabilities. It does not necessarily leave the same way it arrived. To describe the directionality of the scattering in three dimensional space, requires a 3 x 3 matrix or tensor. Because the tensor is symmetric ($\alpha_{yx} = \alpha_{xy}$, $\alpha_{zx} = \alpha_{xz}$, $\alpha_{zy} = \alpha_{yz}$), only six unique elements need be considered. Returning to PtCl_4^{2-} and the D_{4h} character table we find

$$\begin{aligned} \alpha_{xx} + \alpha_{yy} &\approx x^2 + y^2 = a_{1g} \\ \alpha_{xx} - \alpha_{yy} &\approx x^2 - y^2 = b_{1g} \\ \alpha_{xy} &= b_{2g} \\ \alpha_{xz}, \alpha_{yz} &= e_g \\ \alpha_{zz} &= a_{1g} \end{aligned}$$

In D_{4h} the C_4 axis mixes x^2 and y^2 , so that their linear combinations must be used. Such mixing of x^2 and y^2 (as well as x and y , which transform like an e representation) occurs whenever a molecule possesses a C_3 or higher order rotation axis. This tensor symmetry is often referred to as "axial symmetry".

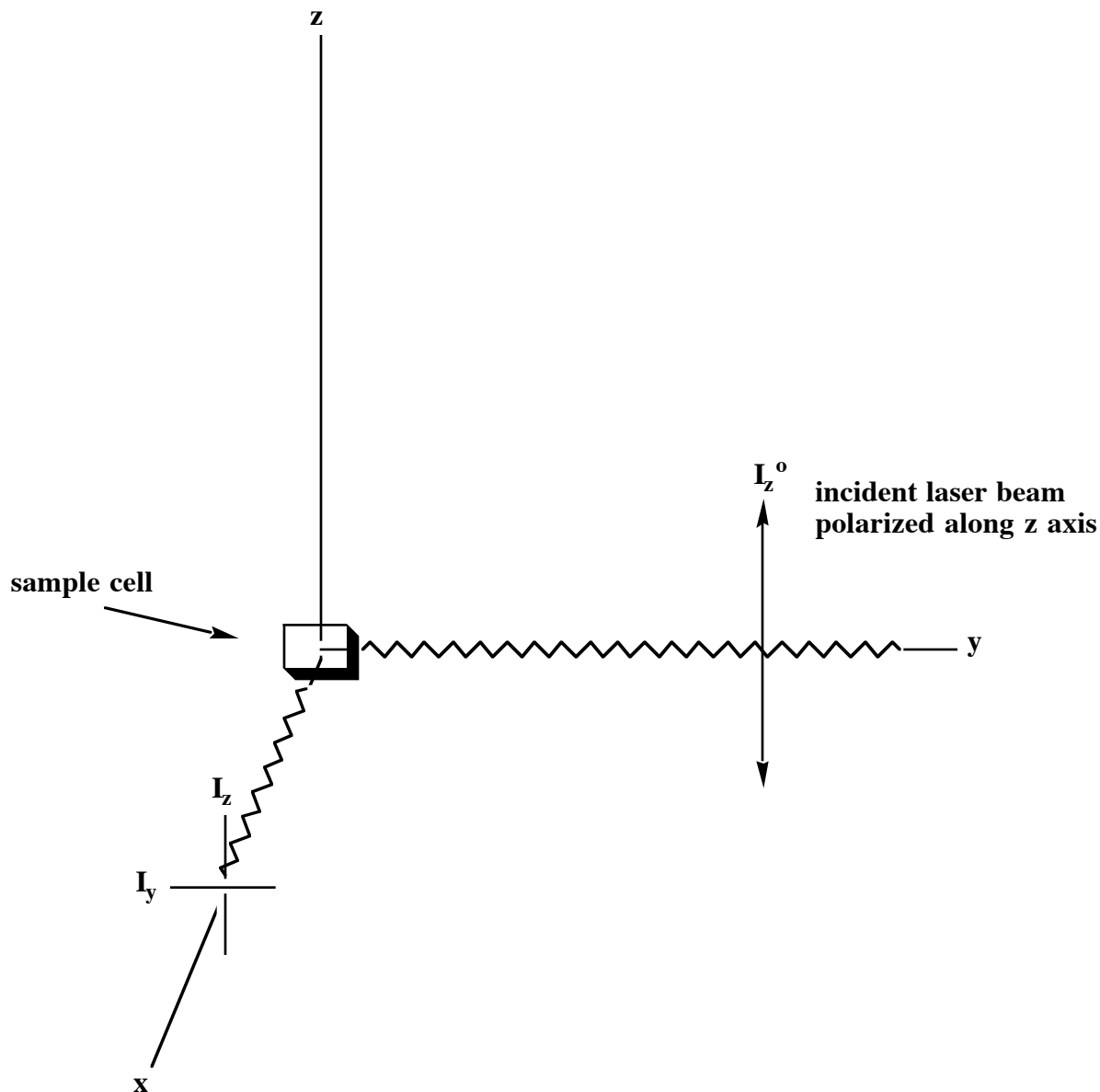


Figure 5.8 Geometry of experiment for measuring the Raman depolarization ratio. The intensity of the z and y polarized components to the scattered radiation can be determined by placing a polarizing filter before the detector.

Selection rules in Raman spectroscopy are determined by the integrals,

$$\langle a_{1g} | \chi_{ij} | \chi_v \rangle \neq 0$$

where $\chi_{ij} = a_{1g}, e_g, b_{1g}$ and b_{2g} , as found above, and χ_v is the irreducible representation for a vibrational symmetry mode. Therefore, the $\chi_k(a_{1g})$, $\chi_4(b_{2g})$ and $\chi_a(b_{1g})$ vibrations in PtCl_4^{2-} should

be observed in the Raman spectrum. The exclusion rule for molecules with a center of symmetry, states that no vibration can be both IR and Raman active. This arises because of the differing symmetries of the polarizabilities (g symmetry) from the dipole moment operators (u symmetry).

One diagnostic tool of use in Raman spectroscopy is the depolarization ratio for liquid or gaseous samples. This experiment is depicted in Figure 5.8. For excitation with a laser polarized along z, the depolarization ratio $\rho = I_y/I_z$ is 3/4 for nontotally symmetric vibrations and $0 \leq \rho < 3/4$ for totally symmetric vibrations, e.g., ν_{a_1g} Mo-Mo in $\text{Mo}_2(\text{O}_2\text{CCF}_3)_4$. The observation of ρ near zero for a particular peak in a spectrum constitutes conclusive proof that it belongs to the totally symmetric representation.

Resonance Raman Spectroscopy. This technique provides a Raman spectrum of enhanced intensity. Certain modes subject to distortion in the excited state may undergo an exceptional (10^5) resonance enhancement relative to other vibrations. This has been used to probe the vibrational spectrum of chromophores in complex biomolecules, such as heme proteins. Often the mode most affected is the totally symmetric one, when the resonant excited state is dipole allowed. The normal modes that experience the resonance effect must be those which undergo a Franck-Condon distortion in the excited state. For example, the Raman spectrum of $\text{Re}_2\text{Cl}_8^{2-}$ in resonance with the $\pi \rightarrow \pi^*$ transition associated with the quadruple metal-metal bond produces a tremendous enhancement of ν_{a_1g} (Re-Re) at 273 cm^{-1} . Up to ten overtones of this vibration have been observed in the spectrum. A small enhancement of the a_{1g} (Re-X) stretch is also observed. See RJH Clark et al JACS **1976**, 98, 2763 and **1975**, 97, 2691.

Application of Vibrational Spectroscopy to the Structure Determination of Metal Carbonyls.

In metal carbonyl complexes, the $\nu(\text{M-C})$ and $\nu(\text{C}\equiv\text{O})$ frequencies are fairly well separated at $400\text{-}600 \text{ cm}^{-1}$ and $1850\text{-}2125 \text{ cm}^{-1}$ (terminal $\text{C}\equiv\text{O}$) or $1700\text{-}1850 \text{ cm}^{-1}$ (doubly bridging CO). Because C-O stretches occur in a region where few other groups absorb, they provide a particularly valuable spectroscopic probe of molecular structure. The task is simple because we need only consider the

nonredundant C-O bond stretching coordinates. Consider the octahedral metal carbonyl complexes of chromium, molybdenum, and tungsten, $M(\text{CO})_6$. Following the usual procedure produces the representation spanned by the C-O stretching coordinates.

$$\begin{array}{rcccccccccc}
 & E & 8C_3 & 6C_2 & 6C_4 & 3C_2=C_4^2 & i & 6S_4 & 8S_6 & 3\sigma_h & 6\sigma_d \\
 \Gamma(\text{C-O}) & 6 & 0 & 0 & 2 & 2 & 0 & 0 & 0 & 4 & 2 \\
 = & & a_{1g} + e_g + t_{1u} & & & & & & & & \\
 & & e_g \text{ Jahn-Teller active vibration} & & & & & & & & \\
 & & & & & & & & & & t_{1u}
 \end{array}$$

Since x, y, z transform like t_{1u} , then $\langle a_{1g} | t_{1u} | \sigma \text{ vib} \rangle \neq 0$ if $\Gamma_{\text{vib}} = t_{1u}$. The $M(\text{CO})_6$ complexes exhibit a single $\Gamma(\text{CO})$ stretch in the IR spectrum. Since $x^2 + y^2 + z^2 = a_{1g}$ and $2z^2 - x^2 - y^2 = e_g$, the a_{1g} and e_g vibrations are Raman active. In octahedral symmetry, t_{2g} vibrations are also Raman allowed; however, the $M(\text{CO})_6$ molecules possess no such vibration. For Cr, Mo, $W(\text{CO})_6$ the solution IR spectrum shows a single intense band at about 1980 cm^{-1} . Carbonyl stretches tend to be the most intense features in the IR spectra of metal complexes and provide a probe of structure. The symmetry situation for the metal-carbon stretching vibrations is entirely analogous to the C-O stretches; however, the low frequency ($350\text{-}450 \text{ cm}^{-1}$) of the M-C stretches allows them to be considered as independent vibrations (Table II), as a rough approximation.

Table II

Summary of $\Gamma(\text{CO})$ and $\Gamma(\text{M-C})$ Stretching Frequencies for $M(\text{CO})_6$ Complexes ($M = \text{Cr, Mo, and W}$) in the Gas Phase

Complex	$\Gamma(\text{C-O}), \text{cm}^{-1}$			$\Gamma(\text{M-C}), \text{cm}^{-1}$		
	t_{1u}	a_{1g}	e_g	t_{1u}	a_{1g}	e_g
$\text{Cr}(\text{CO})_6$	2000.4	2118.7	2026.7	440.5	379.2	390.6
$\text{Mo}(\text{CO})_6$	2000.3	2120.7	2024.8	367.2	391.2	381
$\text{W}(\text{CO})_6$	1997.6	2126.2	2021.1	374.4	426	410

Solvent shifts of $\nu(\text{CO})$ stretching frequencies can amount to 40 cm^{-1} and solid state spectra are much broader than in solution. Best quality spectra are obtained in methylcyclohexane solvent, then alcohols, CCl_4 , and CH_2Cl_2 . Stretching frequencies for the CO ligand often correlate with the amount of electron density donated into the CO π^* orbitals, and hence the π -donor ability of the metal. Consider the isoelectronic series:

$\text{M}(\text{CO})_6$	$\nu_6(t_{1u})$
$\text{Mn}(\text{CO})_6^+$	2094 cm^{-1}
$\text{Cr}(\text{CO})_6$	1984 cm^{-1}
$\text{V}(\text{CO})_6^-$	1858 cm^{-1}

For comparison, free CO absorbs at 2145 cm^{-1} .

In $\text{M}(\text{CO})_5\text{L}$ complexes, such as $\text{HMn}(\text{CO})_5$, $\text{BrRe}(\text{CO})_5$ or $\text{Mo}(\text{CO})_5\text{PPh}_3$, the lowering of symmetry produces more IR active vibrations. These $\text{M}(\text{CO})_5\text{L}$ complexes are treated as follows:

The inequivalent CO groups (axial and equatorial) are considered separately.

	C_{4v}				
	E	$2C_4$	C_2	$2\sigma_v$	$2\sigma_d$
$\nu(\text{CO}_{\text{eq}})$	4	0	0	2	0
$\nu(\text{CO}_{\text{ax}})$	1	1	1	1	1

Therefore

$$\begin{aligned} \nu(\text{CO}_{\text{ax}}) &= a_1 \\ \nu(\text{CO}_{\text{eq}}) &= a_1 + b_1 + e \end{aligned}$$

Since $x, y = E$ and $z = a_1$ there should be 3 IR absorptions. All modes are Raman active, as the C_{4v} character tables shows. For example, $\text{Cr}(\text{CO})_5\text{PH}_3$ exhibits a_1 at 2075 cm^{-1} (m), b_1 at 1982 cm^{-1} as a weak shoulder e, and $a_1 \sim 1953 \text{ cm}^{-1}$ (vs). Although there is a big difference between the a_1 equatorial (2075 cm^{-1}) and e equatorial CO stretch at 1953 cm^{-1} , there is little separation of the axial a_1 and equatorial e stretching vibrations; however, in $\text{Re}(\text{CO})_5\text{Cl}$, $a_1 = 2155 \text{ cm}^{-1}$, $b_1 = 2085 \text{ cm}^{-1}$, $e = 2046 \text{ cm}^{-1}$ and $a_1 = 1983 \text{ cm}^{-1}$ the separation is better. The dipole forbidden b_1 stretch can

sometimes be observed in the IR spectrum. A bothersome feature is that the high frequency a_1 stretch associated with the equatorial CO's is often very weak. We can understand the apparent forbidden character of this allowed stretching vibration by considering the spectrum expected for a $\text{trans } M(\text{CO})_4\text{L}_2$ complex. In D_{4h} symmetry.

$$\begin{array}{ccccccccccc}
 & E & 2C_4 & C_2 & 2C_2' & 2C_2'' & i & 2S_4 & \sigma_h & 2\sigma_v & 2\sigma_d \\
 \nu(\text{C-O}) & 4 & 0 & 0 & 2 & 0 & 0 & 0 & 4 & 2 & 0 \\
 & = & a_{1g} & + & b_{1g} & + & e_u & & & &
 \end{array}$$

Because in D_{4h} $x, y = e_u$ and $z = a_{2u}$, we see that only e_u is IR active. The a_{1g} and b_{1g} vibrations in D_{4h} correlate to the a_1 and b_1 equatorial stretching vibrations in C_{4v} . Therefore, the equatorial a_1 stretch would be forbidden if $M(\text{CO})_4$ group were rigorously coplanar. To the extent that this unit is affected little by the axial substituents, the transition will be approximately forbidden. Another consequence of this reasoning is that the axial a_1 stretch should be most sensitive to the nature of the trans ligand.

Complex	$\nu(\text{Cr-O}), \text{cm}^{-1}$			
	A_1	B_2	E	A_1
$\text{Mn}(\text{CO})_5\text{C}_5\text{F}_4\text{N}^+$	2132	2068	2042	2015
$\text{Mn}(\text{CO})_5\text{SCN}$	2138	2084	2043	1958
$\text{Mn}(\text{CO})_5\text{NCS}$	2141	2113	2053	1958
$\text{Mn}(\text{CO})_5\text{SOMe}_2^+$	2139	2090	~2052	2027
$\Delta\bar{\nu}$	9 cm^{-1}	45 cm^{-1}	10 cm^{-1}	70 cm^{-1}

$M(\text{CO})_4\text{X}_2$ complexes can have *trans*- D_{4h} or *cis*- C_{2v} geometries. An analysis of the possible C-O stretches predicts the following peaks in their vibrational spectra.

D_{4h}			C_{2v}		
IR	-	e_u	IR	-	$2a_1 + b_1 + b_2$
Raman	-	$a_{1g} + b_{1g}$	Raman	-	$2a_1 + b_1 + b_2$

Vibrational spectroscopy allows a clean decision between the two possibilities. One must be careful in the analysis of spectra of metal carbonyls about weak peaks $\sim 40\text{ cm}^{-1}$ lower in energy than an intense IR peak. These often arise from ^{13}C isotopomers. For example, $\sim 7\%$ of $\text{Cr}(\text{CO})_6$ molecules contain one ^{13}CO ligand and the IR spectrum of $\text{Cr}(\text{CO})_6$ shows a weak absorption on the low energy shoulder of the main absorption because of this effect. More complex metal carbonyls structures can often be analyzed by the pseudo symmetry of the $\text{M}(\text{CO})_n$ group. For example cyclopentadienyl manganese tricarbonyl can be treated as containing a $\text{M}(\text{CO})_3$ group of approximate C_{3v} symmetry.

Fig. 5.

For $\text{Fe}_2(\text{CO})_9$, which conforms to D_{3h} symmetry, we consider the 3 equivalent bridging CO's and 6 equivalent terminal CO groups separately.

	E	2C ₃	3C ₂	σ _h	2S ₃	3σ _v
Γ(C-O _b)	3	0	1	3	0	1
	= e' + a ₁ '					

Only e' is IR active and it splits slightly (1855, 1851 cm⁻¹) because of a small deviation from idealized symmetry. For the terminal CO's

Γ(C-O _t)	6	0	0	0	0	2
	= a ₂ ' + e'. These IR active vibrations appear at 2066 and 2038 cm ⁻¹ .					

Application to Metal Hydrides

For diatomic molecules, the bond stretching vibrational frequency for a harmonic oscillator is

$$\bar{\nu} = \frac{1}{2\pi c} \sqrt{\frac{k}{\mu}} \quad \begin{array}{l} k = \text{force constant} \\ \mu = M_1 M_2 / (M_1 + M_2) \end{array}$$

e.g., for CO $k = 18.47 \text{ m dyn}/\text{\AA}$ $\bar{\nu} = 2138 \text{ cm}^{-1}$

for I₂ $k = 1.76 \text{ m dyn}/\text{\AA}$ $\bar{\nu} = 215 \text{ cm}^{-1}$

Force constants are more useful than stretching frequencies, since they correlate roughly with bond strength. Physically $k =$ second derivative or curvature of the potential surface at the equilibrium bond distance. To be written later

Practical IR Spectroscopy:

Table of Infrared Cell Window Materials.

Material	Transmission Range (cm ⁻¹)	Pros and Cons
sodium chloride	625 - UV	Dissolves in water, fogs in air but easily polished to restore
potassium bromide	400 - UV	Softer and more moisture sensitive than NaCl, but a better choice for making pressed pellets (transmits 200 cm ⁻¹ in thin pellets).
calcium fluoride	1100 - UV	Very chemically inert, but brittle and more susceptible to fracture when tightening cells. Inert to most solvents, including aqueous acids and bases (except when NH ₄ ⁺ present. Expensive

Infrared Quartz	2500 - UV	Inert, cheap, but narrow range of usefulness
Sapphire	1800 - UV	Inert like quartz, better transmission, but more expensive
Silver Chloride	400 - 25,000	Water insoluble and better transmission than NaCl, but is photosensitive and soft.
zinc sulfide	715 - 10,000	Only attacked by strong acids, bases, and oxidants. Expensive
Polyethylene	30 - 600 useful for long wavelenth IR	Inert and inexpensive material

Additional Readings

Adams, D. M. *Metal-ligand and Related Vibrations*; St. Martin's Press: New York, 1968.

Birman, J. L. *Theory of Crystal Space Groups and Lattice Dyanmics*; Springer-Verlag: New York, 1984.

Clark, R. J. H.; Hester, R. E., Eds. *Advances in Infrared and Raman Spectroscopy*; 1975.

Colthup, N. B. *Introduction to Infrared and Raman Spectroscopy*, 2d ed; Academic Press: New York, 1975.

Gans, P. *Vibrating Molecules*; Chapman and Hall: London, 1971.

Nakamoto, K. *Infrared and Raman Spectra of Inorganic and Coordination Compounds*; 3rd ed., Wiley: New York, 1978.

Problems:

1) Determine all the vibrations present in CO₂ and N₂O. Sketch the vibrational motions. In the IR spectrum of CO₂ two intense peaks occur at 667 and 2349 cm⁻¹. How would you assign them? For N₂O three intense IR absorptions occur at 598, 1285, and 2224 cm⁻¹. How would you assign these vibrations using the data for CO₂? Nitrous oxide is 200 times as effective as CO₂ as a greenhouse gas. Suggest a reason why.

- 2) Determine all the IR active vibrations and sketch them for the CFC, CF_2Cl_2 , another greenhouse gas.

- 3) Sometimes, in addition to the fundamental IR modes combination and overtones are also observed, which correspond to simultaneous excitation of two vibrations. For N_2O , in addition to the three main IR absorptions, other peaks of medium to weak intensity appear in the spectrum at 1167, 1868, 2461, 2563, 2798, 3366, 3481, 4420, and 4735 cm^{-1} . Can you explain and assign these? Does it make the high greenhouse effect of N_2O as compared to CO_2 easier to explain?

- 4) What is the Boltzmann population of the $\nu = 1$ vibrations for the three fundamentals in N_2O at 300K?

- 5) How many infra red and Raman active vibrations would you expect to see for $\text{Mn}_2(\text{CO})_{10}$ in the C-O stretching frequency region of the spectra if it were a) eclipsed or b) staggered with respect to rotation around the metal-metal bond axis. Sketch the totally symmetric stretching vibration for the staggered geometry.

- 6) How would you expect the IR absorptions for the S-O stretches ($1030 - 1140\text{ cm}^{-1}$) in the sulfate ion to differ for it as a counter ion, as in $[\text{Co}(\text{NH}_3)_6][\text{SO}_4]$, versus when it binds as a monodentate ligand as in $[\text{Co}(\text{NH}_3)_5(\text{SO}_4)][\text{Br}]$?

- 7) Would you be able to distinguish all possible geometric isomers of the trigonal bipyramidal complex $\text{Fe}(\text{CO})_3(\text{PPh}_3)_2$ with a combination of infra red and Raman spectroscopy? Explain your reasoning.

- 8) The perchlorinated hydrocarbon, carbon tetrachloride, is a popular solvent for IR spectroscopy. Why do you think this is so?

- 9) For work in the far infrared ($50 - 200 \text{ cm}^{-1}$) polyethylene windows prove useful in infrared cells. Why do you think this is so?
- 10) What do you think the relative merits would be of using an infrared cell with CaF_2 windows vs. NaCl .
- 11) How might you use vibrational spectroscopy to determine with an oxalate complex $\text{M}(\text{C}_2\text{O}_4)_2$ was square planar or tetrahedral?